

GenMask: Adapting DiT for Segmentation via Direct Mask Generation

Yuhuan Yang^{1,4*} Xianwei Zhuang⁴ Yuxuan Cai^{4†} Chaofan Ma¹ Shuai Bai⁴ Jiangchao Yao^{1,2}
Ya Zhang^{2,3‡} Junyang Lin⁴ Yanfeng Wang^{2‡}

¹Cooperative Medianet Innovation Center, Shanghai Jiao Tong University

²School of Artificial Intelligence, Shanghai Jiao Tong University

³Institute of Artificial Intelligence for Medicine, Shanghai Jiao Tong University School of Medicine

⁴Alibaba Group

Abstract

*Recent approaches for segmentation have leveraged pre-trained generative models as feature extractors, treating segmentation as a downstream adaptation task via indirect feature retrieval. This implicit use suffers from a fundamental misalignment in representation. It also depends heavily on indirect feature extraction pipelines, which complicate the workflow and limit adaptation. In this paper, we argue that instead of indirect adaptation, segmentation tasks should be trained directly in a generative manner. We identify a key obstacle to this unified formulation: VAE latents of binary masks are sharply distributed, noise robust, and linearly separable, distinct from natural image latents. To bridge this gap, we introduce timesteps sampling strategy for binary masks that emphasizes extreme noise levels for segmentation and moderate noise for image generation, enabling harmonious joint training. We present **GenMask**, a DiT trains to generate black-and-white segmentation masks as well as colorful images in RGB space under the original generative objective. **GenMask** preserves the original DiT architecture while removing the need of feature extraction pipelines tailored for segmentation tasks. Empirically, **GenMask** attains state-of-the-art performance on referring and reasoning segmentation benchmarks and ablations quantify the contribution of each component.*

1. Introduction

Text-based segmentation is an important problem in computer vision. It requires the model to predict a binary mask based on natural language descriptions of the image content. With the recent emergence of large-scale self-supervised discriminative pretraining, it is increasingly treated as a downstream adaptation task rather than being learned from scratch. Models such as CLIP [55], trained on web-scale

uncurated data, have demonstrated exceptional capability in capturing high-level visual semantics, thereby offering strong initialization for a variety of segmentation frameworks [21, 27, 44, 46, 71, 77, 84, 89].

Meanwhile, the rapid progress of text based image generation models, especially large scale pretrained latent diffusion models [17, 61], has sparked growing interest, and representations behind them are also widely explored for various of vision tasks including text-based segmentation [30, 66, 78]. Following the paradigm of using discriminative pretrained models, these works typically treat pretrained diffusion generative models as backbones. Segmentation masks are obtained by first extracting hidden features during the denoising or diffusion-inversion process, and then feeding the extracted features into a trainable task-specific decoder [20, 29, 42, 47, 50, 64, 82].

Despite progress, these works still rely on an *implicit use* of pretrained diffusion models, and therefore suffer from two key limitations. **(1)** Diffusion models are pretrained to model the low-level distribution of VAE features, whereas segmentation requires compact, semantic-level label predictions. This representational mismatch hampers effective downstream adaptation. **(2)** Existing methods rely on carefully designed, indirect pipelines to extract features from diffusion models. Common approaches include diffusion inversion [45] and activation aggregation [50, 82]. These intermediate operations also complicate the workflow and limit adaptation performance.

In this paper, we argue that instead of indirect adaptation, *segmentation tasks should be trained directly in a generative manner*. Our method, **GenMask**, realizes this idea by training a Diffusion Transformer (DiT) to directly generate black-and-white segmentation masks in RGB space under a generative training objective. By doing so, we demonstrate three distinct merits. **(1)** Architecturally faithful to the original DiT. The segmentation process can be integrated into the original end-to-end DiT framework without structural changes or extra operations. **(2)** Maximally aligned with the generative training objective. The model continues to be trained under a generative objective, eliminating the op-

*Work done while the author was an intern at Alibaba Group. Email: yangyuhuan@sjtu.edu.cn †Project Leader ‡Corresponding authors. Email: ya_zhang@sjtu.edu.cn, wangyanfeng622@sjtu.edu.cn

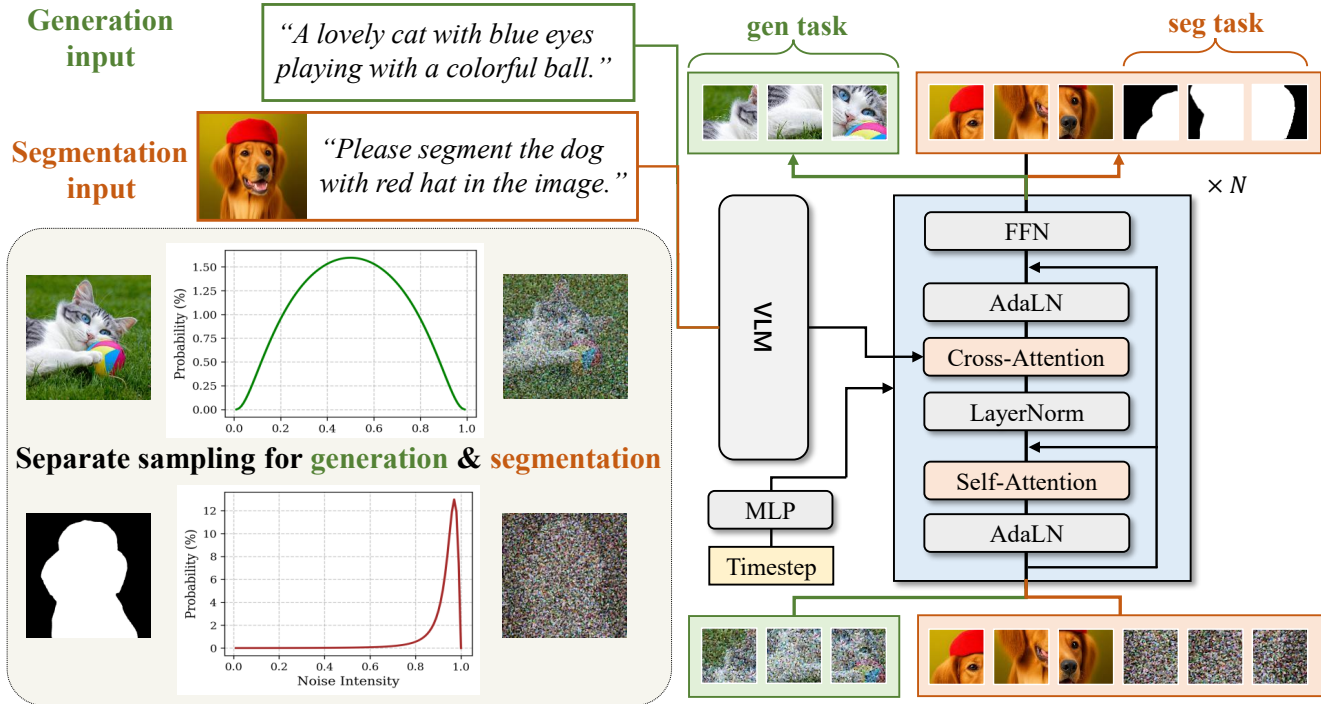


Figure 1. **Overall architecture of our model.** Here **brown** and **green** denote the segmentation and generation data flow respectively. **Generation** task follows standard diffusion training process, and its timesteps sampling strategy is similar to Stable Diffusion 3 [16], emphasizing on intermediate denoising steps. For **segmentation** task, we use an extreme long tailed sampling strategy. We also add VAE representation of the input image into DiT to supplement low-level information for segmentation.

timization gap caused by implicit adaptation. (3) Seamless incorporation of generated data. Generation and segmentation can be trained jointly, allowing the use of generative data to improve segmentation performance.

Specifically, we cast text-to-image generation and text-based segmentation as a single conditional generation objective: the model learns to produce either an image or a segmentation mask with given condition. While pursuing this unified formulation, we discover that *a large gap exists* between the VAE representations of binary segmentation masks and those of natural RGB images. VAE features for RGB images are smooth and easily perturbed by Gaussian noise, whereas features for binary masks are sharply distributed, highly robust to noise, and largely linearly separable. This representational discrepancy makes it difficult for a single generative model to learn both distributions well simultaneously. To address this, we introduce a specific *timesteps sampling strategy* for segmentation masks: we sample extremely high noise levels more frequently, while for generation examples we emphasize moderate noise levels. This tailored sampling lets the model capture the two distinct feature distributions effectively. We further optimize the inference pipeline to produce masks with a single model forward pass. As a result, we obtain a deterministic segmentation model trained under the same generative objective in pretraining.

Based on this solution, we build our model on a pre-trained DiT and employ a vision-language model (VLM) to encode both visual and textual instructions for generation and segmentation. For segmentation, we also inject the input image’s VAE latent as a low-level shortcut to provide the texture and color cues needed for accurate pixel-level prediction. Beyond achieving state-of-the-art results on referring and reasoning segmentation benchmarks, we also present comprehensive empirical studies that quantify the contribution of each key component in our architecture.

2. Method

We first provide the necessary preliminaries on the diffusion algorithm and model architecture in Sec. 2.1. Then, Sec. 2.2 presents our key contribution: sampling strategy that integrates binary segmentation mask into the conventional low-level visual sampling process of the diffusion model. Finally we introduce the detailed implementation of our architecture in Sec. 2.3, describing how we harmonize the discriminative segmentation task with the low-level visual generation dynamics in a unified learning paradigm.

2.1. Overview

Preliminaries on Flow Matching. Flow Matching [34] is a generative modeling framework that learns a continuous

path to transform simple noise (e.g., Gaussian) into complex data (e.g., natural images). An effective version of Flow Matching is Rectified Flow [41]. Instead of using complex paths, it trains the model with the simplest one: a straight line between data and noise. Concretely, for each image \mathbf{x}_0 and a random Gaussian noise $\epsilon \sim N(0, \mathbf{I})$, we define a linear path that connects \mathbf{x}_0 to ϵ with a constant direction vector $\mathbf{v} = \mathbf{x}_0 - \epsilon$ over the time interval $t \in [0, 1]$:

$$\mathbf{x}_t = \mathbf{x}_0 - t \cdot \mathbf{v} = t\epsilon + (1 - t)\mathbf{x}_0. \quad (1)$$

The goal of Rectified Flow is to train a neural network $v_\theta(\mathbf{x}_t, t)$ to predict the direction vector \mathbf{v} . And the loss is defined as:

$$\mathcal{L}(\theta) = \mathbb{E}_{\mathbf{x}_0, \epsilon, t} \|\mathbf{x}_0 - \epsilon - v_\theta(\mathbf{x}_t, t)\|^2. \quad (2)$$

Architecture Overview. GenMask integrates both text-to-image generation and language-guided segmentation tasks in one framework without additional parameter. As illustrated in Fig. 1, both tasks rely on the same diffusion training process. The only variation between them is the timesteps sampling schedule: segmentation uses an aggressively long-tailed distribution to focus learning on the high-noise region.

2.2. Timesteps Sampling for Segmentation Masks

Natural images contain rich textures, diverse colors, and fine-grained details, whereas binary segmentation masks contain only sparse foreground-background patterns and possess extremely low visual complexity. Due to this discrepancy, the latent space of masks occupies a narrow, highly biased region, making it difficult for generative models trained on natural-image distributions to model mask statistics reliably. Such distributional mismatch also underlies the limitations of previous diffusion model based segmentation approaches. In this section, we first highlight this inherent bias and then present our timesteps sampling strategy for segmentation mask to address this challenge. Specifically, in Sec. 2.2.1, we examine in detail how the distribution of segmentation masks differs from that of natural images. Then, in Sec. 2.2.2, we review the widely adopted timesteps sampling strategy for image generation. Finally we introduce our sampling strategy for segmentation task in Sec. 2.2.3. By *separating general image denoising and mask denoising into different timesteps with different noise intensity*, the model can learn two tasks simultaneously with a unified architecture and training objective.

2.2.1. Latent Distribution for Binary Masks

We starts from a demo example by visualizing the process of adding noise to a natural image and a binary mask in Fig. 2. Interestingly, we find that *binary masks are much more robust to noise* than natural images. For a natural

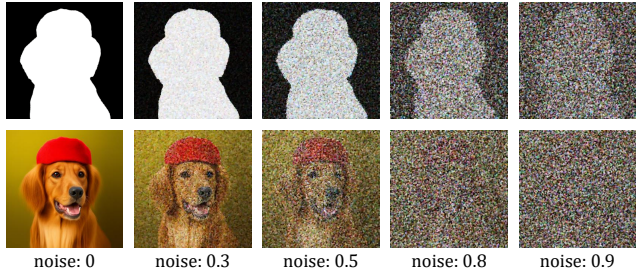


Figure 2. **The process of adding noise to natural image and binary mask.** Compared with natural image, binary mask is much more robust to noise.

image, introducing an extremely high level of noise completely obliterates its content, making the result almost indistinguishable from random noise. In contrast, when the same noise level is applied to a binary segmentation mask, the global position and shape of the segmented region remain largely intact, even the boundaries remain clearly recognizable. These observations suggest that the latent representations of binary masks may be fundamentally different from those of natural images.

To further understand this phenomenon, we analyze a toy example and uncover a simple yet often overlooked fact: *the VAE representation of binary segmentation masks is effectively linearly separable.* We randomly sample N segmentation masks from our dataset, and encode them into VAE representation with shape $\mathbf{X} \in \mathbb{R}^{N \times hw \times d}$. Here $d = 16$ is the VAE latent dimension. We see \mathbf{X} as $N \times hw$ data, and perform PCA decomposition into only ONE principal component, and gets $\mathbf{Y} = \mathbf{X}\mathbf{W} \in \mathbb{R}^{N \times hw}$. The whole process is shown as:

$$\text{Binary Mask } N \times HW \rightarrow \text{VAE Feature } N \times hw \times d \rightarrow \text{PCA Label } N \times hw \quad (3)$$

We take $N = 100$ and shows 6 of the input mask and output the visualization for both segmentation mask and PCA label in Fig. 3. We find the PCA label is extremely similar with input mask, which means, the VAE representation space is linear separable with \mathbf{W} .

Finally, we gradually add noise to the VAE representation of the input mask and use least squares classification for label regression. The validation accuracy is shown in Fig. 4. The results reveal that only at high noise intensity does the linear separability collapse, providing meaningful information for segmentation.

2.2.2. Time Shift for Generation

The non-uniform importance of denoising steps has been studied for image generation task. For generation task, early timesteps (dominated by noise) and late timesteps (concerned only with fine details) provide limited useful learning signals. Stable Diffusion 3 (SD3) [16] proposes

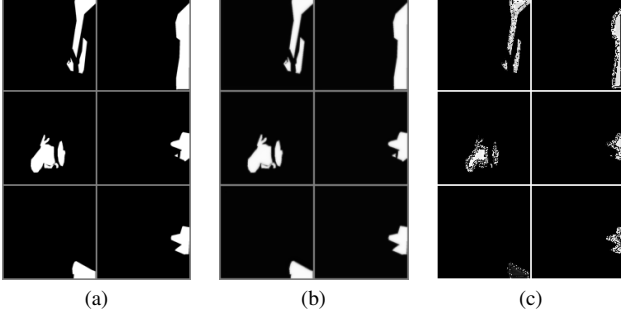


Figure 3. VAE features for binary segmentation masks are linearly separable. (a) The input segmentation masks. (b) PCA label of its VAE representation. (c) The difference between the input masks and the PCA label after histogram normalization.

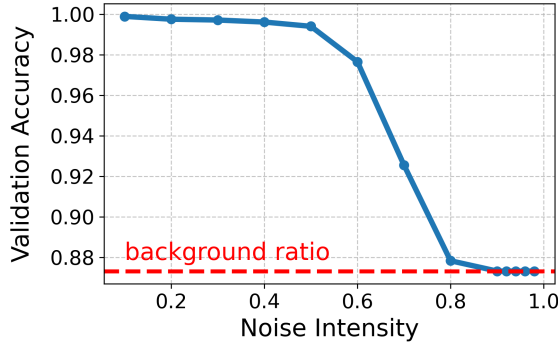


Figure 4. SVM validation accuracy on VAE embeddings of binary masks under different noise levels. The embeddings remain linearly separable under low noise, while only high-intensity perturbations substantially degrade separability.

a resolution-dependent timesteps sampling strategy. Following SD3, we use the logit-normal sampling strategy to emphasize intermediate noise levels during training. The probability density function of timestep t is given by:

$$\pi(t) = \frac{1}{\sqrt{2\pi t(1-t)}} \exp\left(-\frac{1}{2} \left[\log\left(\frac{t}{1-t}\right)\right]^2\right). \quad (4)$$

In practice, we sample the random variable u from a normal distribution $u \sim \mathcal{N}(0, 1)$, and then transform it to timestep t using the inverse of the cumulative distribution function:

$$t = \frac{1}{1 + e^{-u}}. \quad (5)$$

2.2.3. Time Shift for Segmentation

Inspired by the timesteps sampling strategy for generation task, we propose that segmentation task also needs a tailored sampling strategy during training to ensure effectiveness. This sampling strategy should be long tailed, and concentrate in the high noise intensity regime. Here we construct a probability density function $p(t)$ with extreme long

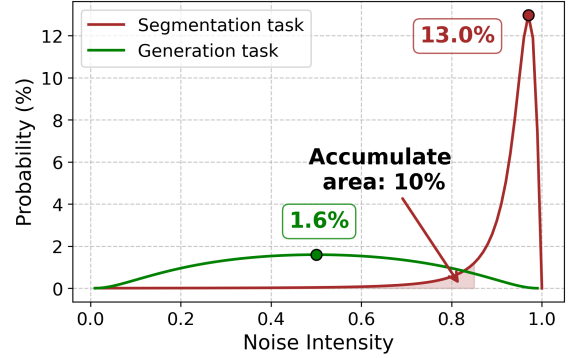
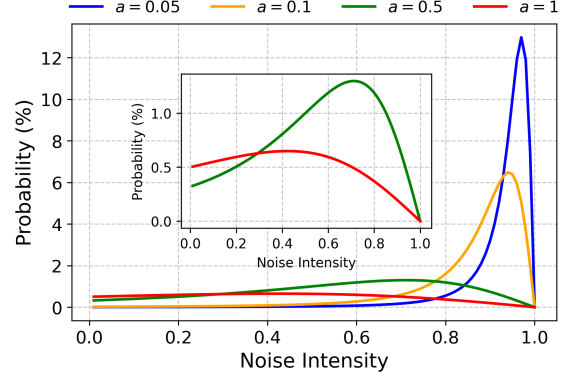


Figure 5. (Up) Importance resampling function for segmentation task with different hyperparameter a . More extreme a value means the distribution is more concentrated in high noise intensity regime. (Down) Different sampling strategies for segmentation and generation task separately. Generation task uses a relatively uniform sampling strategy, only emphasize the intermediate denoising steps. While segmentation task uses a extreme long tailed sampling strategy, with peak value $8\times$ higher.

tail in early timesteps:

$$p(t) = \frac{2a^2t}{(t^2 + a^2)^2}. \quad (6)$$

And in practice, we first sample the uniform distributed random variable $u \sim \mathcal{U}(0, 1)$, and then transform it via:

$$t = \sqrt{\frac{u}{1-u}} \cdot a, \quad (7)$$

where a is a hyperparameter about time shift. Fig. 5 (Up) shows the distribution curve with different a . Smaller a means the distribution is more concentrated in high noise intensity regime. We draw the two sampling strategies from Eq. (4) and Eq. (6) together in Fig. 5 (Down), and observe that the noise distributions for the two tasks are completely different. The generation task adopts a near-uniform sampling strategy, where the probability mass around the intermediate noise region is only slightly elevated, resulting in a modest peak of 1.6%. This mild adjustment essentially equivalent to adding a small weight to mid-range timesteps during training [16]. By contrast, the segmentation task

relies on an extremely long-tailed distribution with a pronounced peak of 13%, over 8× higher than that of the generation task. The cumulative probability below $t = 0.85$ is merely 10%, meaning that 90% of training samples are intentionally concentrated in the high-noise region.

2.2.4. One-step Inference for Segmentation

Since the segmentation task is trained predominantly on high-noise-intensity timesteps, low-noise regions provide only limited discriminative information for mask prediction. This property allows us to bypass the multi-step progressive denoising steps, which are typically required in diffusion inference. During inference, we fix the sampling timestep $t = 1$, the segmentation mask is generated with only one model forward pass:

$$x_{\text{mask}} = \epsilon + v(\epsilon, 1). \quad (8)$$

Finally, we decode the latent representation x_{mask} with VAE decoder to get the final mask.

Remarkably, in usage pattern, this one-step decoding process aligns perfectly with those conventional, carefully designed segmentation decoders, yet it requires no changes in original diffusion network architecture or additional training parameters. This reveals an appealing property of our model: despite with purely generative training objective, it naturally yields deterministic and accurate segmentation, aligning seamlessly with the demands of real-world deployment.

2.3. Model Architecture and Training Objectives

GenMask is built upon the pretrained WAN-2.1 DiT [68] architecture. Fig. 1 illustrates the overall architecture of our proposed model.

DiT Decoder. WAN-2.1 is a cross-attention based DiT. It accepts the noisy image as input, then uses cross-attention mechanism to integrate the conditional information, and outputs the denoised image. Besides, it also uses AdaLN operation [53, 86] to inject time embedding into the denoising process.

VLM as Instruction Encoder. WAN-2.1 originally uses umT5 [12] as its instruction encoder. However, segmentation task needs to encode both images and text instructions, while umT5 is only capable of text encoding. Thus, we replace the umT5 with an open-source vision-language model (VLM), Qwen2.5-VL-7B [1], to encode instructions for both image generation and segmentation tasks. Specifically, for the segmentation task, the input instruction is formatted as follows:

“[Image]. Please segment the {target} in the image.”

We extract the hidden states from its final layer to serve as the conditional input for the subsequent diffusion model.

VAE as Low-level Representation. VLMs primarily capture high-level semantic features, while segmentation tasks

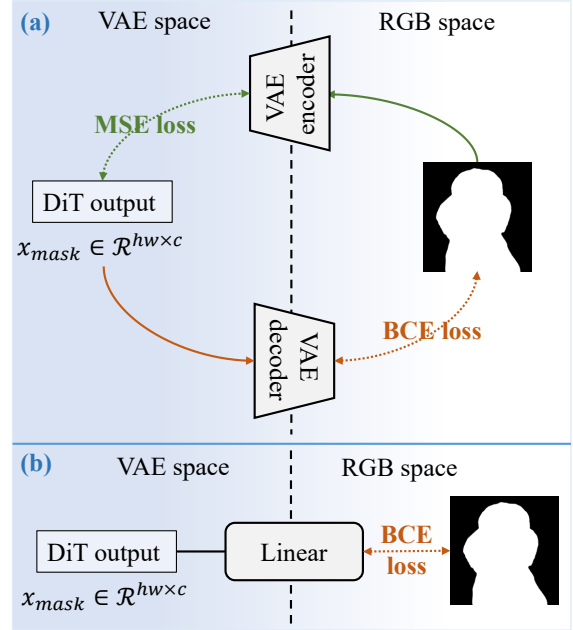


Figure 6. **Three variants of segmentation supervision formats.** (a) MSE loss in VAE space or BCE loss in RGB space with the help of VAE encoder-decoder. (b) By replacing the VAE decoder with a linear layer, we can apply BCE loss without backpropagation through frozen VAE.

require low-level information such as texture and color connectivity for accurate pixel-level prediction. Inspired from those image editing models [3, 39] which use VAE representation as a low-level shortcut, we introduce an additional VAE feature of the input image into DiT for segmentation task specifically. This latent representation is concatenated with randomly sampled noise to form the DiT’s input. We set the time embedding of the raw VAE representation to zero during AdaLN layer, indicating that it represents a completely clean (i.e., noise-free) image.

Training Objective. Generative models commonly use mean squared error (MSE) in Eq. (2) for training, while binary segmentation tasks are typically optimized with binary cross-entropy (BCE) in label space. In this work we explore both supervision strategies and find MSE to be the preferred choice. It’s simple to apply, incurs no extra decoder gradient flow, and tends to produce stronger results.

By contrast, applying BCE naively requires decoding VAE latents back to RGB and computing segmentation logits in pixel space, which forces gradients to flow through the VAE decoder. This is inefficient and adds substantial computational overhead. As discussed in Sec. 2.2.1, VAE latents for segmentation masks are largely linearly separable. Motivated by this, we propose a third variant that replaces the VAE decoder with a simple learnable linear projection and applies BCE directly after this projection. This change removes the need to back-propagate through the full VAE decoder while preserving the ability to train with BCE. It

also speeds up inference, since producing a mask only requires a single linear forward pass instead of the full decoder. Fig. 6 illustrates these three supervision pipelines; their comparative performance is analyzed in the ablation study Sec. 3.3.

CFG Process During Training & Inference. Classifier-Free Guidance (CFG) is a conditioning technique that combines conditional and unconditional diffusion model scores to strengthen adherence to the conditioning signal without requiring an external classifier [23]. However, segmentation is inherently a deterministic prediction problem and therefore does not benefit from CFG. As a result, we apply CFG only to natural-image generation during training, while segmentation samples remain strictly conditioned on the input image and textual instruction. This design, in turn, allows segmentation masks to be produced with a single forward pass, eliminating the need for the dual conditional-unconditional evaluations required by CFG.

3. Experiments

Implementation Details. Our framework is built upon the open sourced WAN-2.1 DiT model with 1.3B parameters [68] and Qwen2.5-VL-7B VLM [1]. VLM and VAE encoder-decoders are kept frozen during training, while the whole DiT model is finetuned end-to-end with both segmentation and generation data. We use cosine decay learning rate scheduler with initial learning rate 5e-5 and minimum learning rate 1e-5. Most training settings converge around 8000 iterations with global batch size of 1024. Segmentation and generation tasks are mixed with 1:1 ratio.

Training Recipe. Our training recipe contains three types of data: semantic segmentation, referring segmentation, and text-to-image generation. **(1) Semantic segmentation:** We use the COCO-stuff [5], ADE20K [93] and Pascal3D+ [18] dataset for semantic segmentation. These parts of data are reformatted into binary segmentation masks follow LISA [28]. **(2) Referring segmentation:** We use the RefCOCO, RefCOCO+ [26] and RefCOCO-g [51] dataset for referring segmentation. **(3) Text-to-image generation:** We use open-sourced datasets such as DiffusionDB [72], BLIP-3o series [8] as well as data provided from third party for text-to-image generation.

Evaluation Metrics. Following conventions [14, 87], we evaluate our model on widely used referring segmentation benchmark RefCOCO series [14, 49, 87], using mIoU and oIoU metrics. We also report results on ReasonSeg [28].

3.1. Comparison with State-of-the-art Methods

Referring Segmentation Results. Here we compare the performance of our approach with several state-of-the-art methods on referring segmentation benchmarks. The results are summarized in Tab. 1, where we demonstrate the

effectiveness and competitiveness of our model relative to existing approaches.

Table 1. **Performance comparison on RES benchmarks.** The results are evaluated on RefCOCO, RefCOCO+ [26], and RefCOCOg [51] (UMD partition) using mIoU and oIoU.

Method	RefCOCO test A / B	RefCOCO+ test A / B	RefCOCO-g val / test
<i>Metric: oIoU</i>			
CRIS [71]	71.5 / 62.2	64.1 / 48.4	56.6 / 57.4
VLT [14]	76.0 / 69.6	68.4 / 56.9	63.5 / 66.2
LAVT [87]	75.8 / 68.8	68.4 / 55.1	61.2 / 62.1
BKINet [15]	76.4 / 69.4	69.9 / 53.4	64.2 / 63.8
ReLA [35]	76.5 / 70.2	71.0 / 57.7	65.0 / 66.0
SLViT [52]	76.9 / 70.6	69.3 / 56.1	62.8 / 63.6
SADLR [88]	76.3 / 70.1	69.1 / 55.2	63.6 / 63.6
DMMI [25]	77.1 / 70.2	69.7 / 57.0	63.5 / 64.2
CGFormer [65]	77.3 / 70.6	71.0 / 57.1	64.7 / 64.1
RISCLIP [27]	76.5 / 69.8	70.6 / 55.5	64.1 / 65.1
MagNet [11]	78.2 / 71.1	71.3 / 58.1	65.4 / 66.0
LQMFormer [62]	76.8 / 71.0	71.8 / 57.6	64.7 / 66.0
ReMamber [85]	76.7 / 70.9	70.8 / 57.5	63.9 / 64.0
MAGNET [11]	78.3 / 72.2	73.6 / 61.8	67.8 / 69.3
PolyFormer-L [36]	78.3 / 73.3	74.6 / 61.9	69.2 / 70.2
UNINEXT-L [80]	82.6 / 77.8	74.9 / 62.6	73.4 / 73.7
LISA [28]	79.1 / 72.3	70.8 / 58.1	67.9 / 70.6
GLaMM [57]	83.2 / 76.9	78.7 / 64.6	74.2 / 74.9
u-LLaVA [79]	82.7 / 77.8	76.6 / 66.8	74.8 / 75.6
PSALM [91]	78.1 / 76.6	70.7 / 64.4	71.0 / 72.3
GSVA [74]	80.4 / 74.2	71.5 / 60.9	74.2 / 75.6
PixelLM [59]	76.5 / 68.2	71.7 / 58.3	69.3 / 70.5
GenMask (Ours)	83.3 / 79.4	78.7 / 68.1	75.6 / 76.5
<i>Metric: mIoU</i>			
EEVG [9]	79.6 / 75.3	75.6 / 64.6	71.5 / 71.9
PromptRIS [63]	81.2 / 74.6	76.6 / 64.3	69.2 / 70.5
OneRef-B [76]	81.9 / 77	77.9 / 69.6	74.1 / 74.9
C3VG [13]	82.9 / 79.1	79.6 / 72.4	76.3 / 77.1
GenMask (Ours)	83.7 / 80.7	80.0 / 73.1	77.2 / 78.2

Reasoning Segmentation Results. Since our encoder is based on a vision-language model (VLM), it can also handle reasoning tasks as well. To fully leverage the VLM’s reasoning capabilities during inference, we adopt a multi-stage pipeline. In the first stage, both the images and the instructions are provided to the VLM. The VLM outputs a clarified and more specific description of the target object to be segmented. In second stage, the refined instruction, together with the original image, is then passed to the DiT for segmentation inference. Tab. 2 shows the performance of our model on ReasonSeg benchmarks.

3.2. Visualization

The visualization results of our model are presented in Fig. 7, demonstrating its capability to simultaneously gen-

Table 2. **Performance comparison on ReasonSeg benchmarks.** Here * denotes the model finetuned on ReasonSeg training dataset.

Model	Val Set		Test Set	
	gIoU	cIoU	gIoU	cIoU
SEEM [95]	25.5	21.2	24.3	18.7
Grounded SAM [58]	26.0	14.5	21.3	16.4
OVSeg [33]	28.5	18.6	26.1	20.8
GLaMM [56]	47.4	47.2	–	–
SAM4MLLM [10]	46.7	48.1	–	–
LISA [28]	44.4	46.0	36.8	34.1
LISA* [28]	52.9	54.0	47.3	34.1
Ours	51.1	50.9	52.3	45.8

erate both colorful images and binary masks. For the segmentation outputs, the predicted binary masks are overlaid on the original images for clearer visualization.

3.3. Ablation Studies

Sampling Strategy. We conduct an ablation study on the sampling strategy for the segmentation task by adjusting the hyperparameter a in Eq. (6) which controls the degree of concentration towards the tail of the distribution. Fig. 5 illustrates the sampling distributions for different values of a . Specifically, we experiment with $a \in [0.05, 0.1, 0.5]$.

Table 3. **Performance comparison of different sampling strategies for segmentation task.** Adjusting segmentation sampling strategy to differ from generation is essential. A relatively smooth distribution (larger a) leads to degraded model performance, whereas the most extreme long-tailed distribution ($a = 0.05$) achieves the best results.

a value	RefCOCO		RefCOCO+		RefCOCO-g	
	mIoU	oIoU	mIoU	oIoU	mIoU	oIoU
0.05	82.2	81.3	75.8	73.5	77.7	76.0
0.1	78.1	77.6	69.3	68.1	73.7	72.3
0.5	66.0	66.0	52.7	53.3	57.5	56.6

The experimental results in Tab. 3 highlight that adapting the sampling strategy is essential for the effective training of the segmentation model. While a larger a ($a = 0.5$) produces a smooth sampling distribution akin to generative training, it leads to the poorest performance. In contrast, a more long-tailed distribution ($a = 0.1$) substantially improves results, with the most extreme strategy ($a = 0.05$) achieving the best performance. This demonstrates that emphasizing high-noise samples is crucial for effective segmentation training.

Segmentation Supervision Format. As discussed in Sec. 2.3, we propose three variants of segmentation supervision formats. Fig. 6 shows the pipeline of these three variants. Tab. 4 summarizes the performance. (1) We find that using MSE loss in the VAE space yields the best results,

since it’s the most closely aligned one with the original DiT training objective, thereby minimizing the need for additional adaptation. (2) Directly applying BCE loss in RGB space produces only moderate results. That’s because, although the VAE encoder and decoder are kept frozen, applying BCE loss in the RGB space still requires backpropagation through the VAE, which makes optimization more difficult and reduces training efficiency. (3) Replacing the VAE decoder with a linear layer alleviates the optimization difficulty, but the performance still falls short of the MSE loss approach.

Table 4. **Performance comparison of different segmentation supervision formats.** MSE performs best since it’s the most closely aligned with the original DiT training objective. Raw BCE performs poorly because it requires backpropagation through VAE, making optimization more difficult. Replacing the VAE decoder with a linear layer alleviates the optimization difficulty.

Loss	RefCOCO		RefCOCO+		RefCOCO-g	
	mIoU	oIoU	mIoU	oIoU	mIoU	oIoU
MSE	82.2	81.3	75.8	73.5	77.7	76.0
BCE	78.1	77.6	73.1	70.3	75.0	72.2
BCE w/ linear	81.3	80.4	74.8	72.4	76.9	75.0

Mix Training. Since our approach formulates the segmentation task within a generative training framework, data used for training generative models can be seamlessly integrated into the segmentation training stage. Consequently, we introduce text-to-image data at a 1:1 ratio for joint training. As shown in Tab. 5, this incorporation of generative data leads to a positive improvement. The results indicate that such data augmentation is beneficial to segmentation performance, suggesting that the gap between generative modeling and segmentation may be less pronounced.

Table 5. **Ablation study on mix training.** Adding generation data in an 1:1 ratio is beneficial to segmentation performance.

Gen data	RefCOCO		RefCOCO+		RefCOCO-g	
	mIoU	oIoU	mIoU	oIoU	mIoU	oIoU
✓	82.2	81.3	75.8	73.5	77.7	76.0
×	81.0	80.6	74.2	72.4	76.7	75.0

VAE Shortcut for Segmentation. Segmentation is actually a task that requires on low-level information, whereas the VLM component mainly captures semantic-level information. Therefore, we introduce a VAE-encoded image latent representation into the input of DiT to incorporate low-level features. As shown in Tab. 6, the segmentation performance deteriorates significantly when the VAE input is removed. This marked decline underscores the critical role of low-level information provided by the VAE encoder.

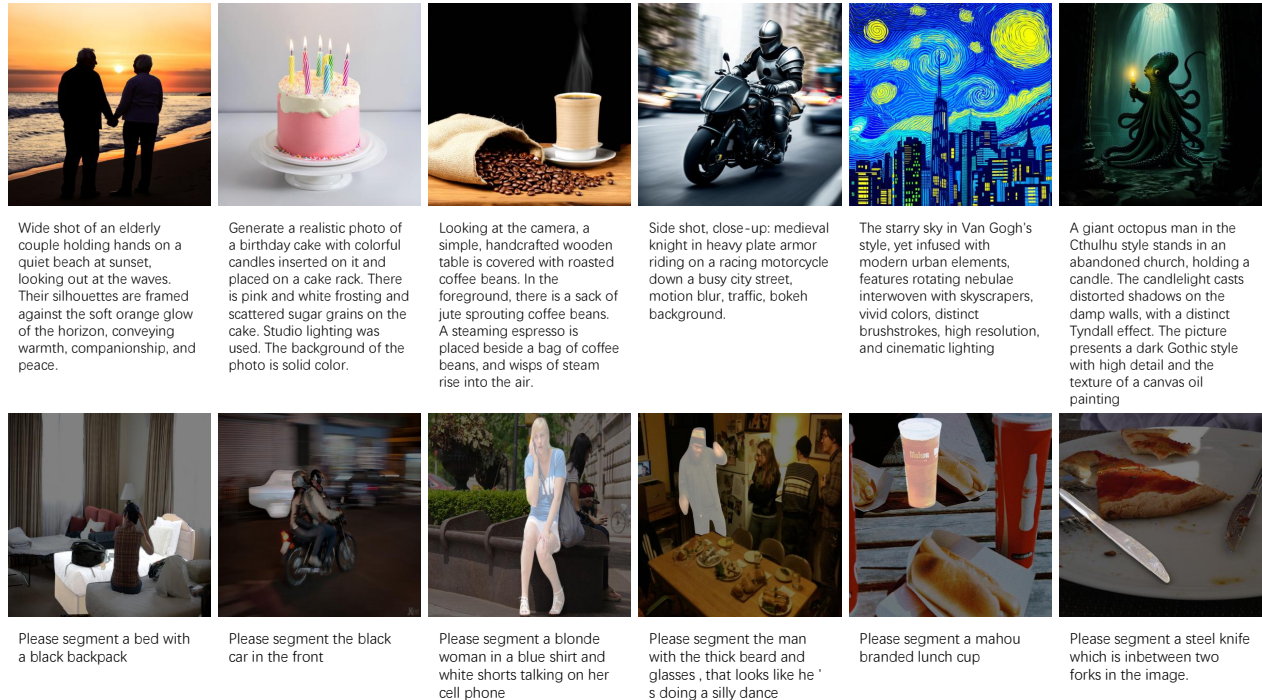


Figure 7. **Visualization results of our model.** We are able to generate both colorful images (up) and binary masks (down) simultaneously. For segmentation, we apply the output binary mask on the original image for better visualization.

Table 6. **Ablation study on VAE input for segmentation task.** VAE input is crucial for segmentation task, it provides low-level information which is essential for accurate pixel-level prediction.

VAE	RefCOCO		RefCOCO+		RefCOCO-g	
	mIoU	oIoU	mIoU	oIoU	mIoU	oIoU
✓	82.2	81.3	75.8	73.5	77.7	76.0
×	74.1	73.2	68.8	67.6	72.4	71.1

4. Related Work

Latent Diffusion Models and Their Representations. Latent Diffusion Models (LDM) [24, 54, 60] perform diffusion in a compressed latent space, greatly improving generation quality and efficiency. Recent advances replace U-Net denoisers with transformers [7, 16, 53], scaling successfully to text-to-image [2, 6], text-to-video [4, 22], as well as unified generation and editing frameworks [3, 69, 70, 73].

Beyond generation, a growing body of work reveals that diffusion models also learn powerful representations [19]: intermediate features exhibit strong discriminative ability [30, 75], hybrid architectures jointly handle generation and recognition [67, 83], and distillation pipelines transfer such representations to downstream tasks [32, 81].

Generative Models for Segmentation. DatasetGAN [90] and BigDatasetGAN [31] use GANs as labeled-data factories, producing unlimited image-mask pairs from a few an-

notations. With the rise of diffusion models, many works extract their internal features for segmentation via frozen feature decoding [78, 92], diffusion inversion [45], multi-step activation aggregation [29, 42, 50], or feature distillation [20, 64]. These methods all treat diffusion models as implicit feature backbones with external decoders, leaving a gap with the generative pretraining objective.

5. Conclusion

We present **GenMask**, which argues for training segmentation in a generative style, by directly treating mask production as a conditional generation problem. Our investigation reveals that the VAE latents of binary masks differ from those of natural images, and we bridge this gap by introducing a separate timestep sampling strategy that enables conflict-free joint training of segmentation and generation. This formulation removes bespoke feature extraction pipelines, closes the optimization gap between pretraining and downstream adaptation, and naturally incorporates generated data to benefit segmentation. Experiments on referring and reasoning segmentation benchmarks demonstrate **GenMask**'s state-of-the-art performance. Future work includes scaling the approach to larger DiT backbones and extending this unified generative paradigm to broader visual and multimodal tasks, such as medical image segmentation [40, 43, 48] and audio-visual segmentation [37, 38, 94].

Acknowledgments

This work is supported by National Key R&D Program of China (No. 2022ZD0160702), National Natural Science Foundation of China (No. 62306178), STCSM (No. 22DZ2229005), 111 plan (No. BP0719010).

References

- [1] Shuai Bai, Keqin Chen, Xuejing Liu, Jialin Wang, Wenbin Ge, Sibao Song, Kai Dang, Peng Wang, Shijie Wang, Jun Tang, et al. Qwen2.5-vl technical report. *arXiv preprint arXiv:2502.13923*, 2025. 5, 6
- [2] James Betker, Gabriel Goh, Li Jing, Tim Brooks, Jianfeng Wang, Linjie Li, Long Ouyang, Juntang Zhuang, Joyce Lee, Yufei Guo, Wesam Manassra, Prafulla Dhariwal, Casey Chu, Yunxin Jiao, and Aditya Ramesh. Improving image generation with better captions. *OpenAI Technical Report*, 2023. 8
- [3] Black Forest Labs, Stephen Batifol, Andreas Blattmann, Frederic Boesel, Saksham Consul, Cyril Diagne, Tim Dockhorn, Jack English, Zion English, Patrick Esser, Sumith Kulal, Kyle Lacey, Yam Levi, Cheng Li, Dominik Lorenz, Jonas Müller, Dustin Podell, Robin Rombach, Harry Saini, Axel Sauer, and Luke Smith. Flux.1 kontext: Flow matching for in-context image generation and editing in latent space. *arXiv preprint arXiv:2506.15742*, 2025. 5, 8
- [4] Tim Brooks, Bill Peebles, Connor Holmes, Will DePue, Yufei Guo, Li Jing, David Schnurr, Joe Taylor, Troy Luhman, Eric Luhman, Clarence Ng, Ricky Wang, and Aditya Ramesh. Video generation models as world simulators. Technical report, OpenAI, 2024. 8
- [5] Holger Caesar, Jasper Uijlings, and Vittorio Ferrari. Cocosuff: Thing and stuff classes in context. In *Proceedings of the IEEE conference on computer vision and pattern recognition*, pages 1209–1218, 2018. 6
- [6] Junsong Chen, Chongjian Ge, Enze Xie, Yue Wu, Lewei Yao, Xiaozhe Ren, Zhongdao Wang, Ping Luo, Huchuan Lu, and Zhenguo Li. Pixart- Σ : Weak-to-strong training of diffusion transformer for 4k text-to-image generation. In *European Conference on Computer Vision (ECCV)*, 2024. 8
- [7] Junsong Chen, Jincheng Yu, Chongjian Ge, Lewei Yao, Enze Xie, Yue Wu, Zhongdao Wang, James T. Kwok, Ping Luo, Huchuan Lu, et al. Pixart- α : Fast training of diffusion transformer for photorealistic text-to-image synthesis. In *International Conference on Learning Representations (ICLR)*, 2024. 8
- [8] Jiu hai Chen, Zhiyang Xu, Xichen Pan, Yushi Hu, Can Qin, Tom Goldstein, Lifu Huang, Tianyi Zhou, Saining Xie, Silvio Savarese, Le Xue, Caiming Xiong, and Ran Xu. Blip3-o: A family of fully open unified multimodal models-architecture, training and dataset. *arXiv preprint arXiv:2505.09568*, 2025. 6
- [9] Wei Chen, Long Chen, and Yu Wu. An efficient and effective transformer decoder-based framework for multi-task visual grounding. In *European Conference on Computer Vision*, pages 125–141. Springer, 2024. 6
- [10] Yi-Chia Chen, Wei-Hua Li, Cheng Sun, Yu-Chiang Frank Wang, and Chu-Song Chen. Sam4mllm: Enhance multimodal large language model for referring expression segmentation. In *European Conference on Computer Vision (ECCV)*, 2024. 7
- [11] Yong Xien Chng, Henry Zheng, Yizeng Han, Xuchong Qiu, and Gao Huang. Mask grounding for referring image segmentation. In *Proceedings of the IEEE/CVF Conference on Computer Vision and Pattern Recognition*, pages 26573–26583, 2024. 6
- [12] Hyung Won Chung, Noah Constant, Xavier Garcia, Adam Roberts, Yi Tay, Sharan Narang, and Orhan Firat. Unimax: Fairer and more effective language sampling for large-scale multilingual pretraining. In *International Conference on Learning Representations (ICLR)*, 2023. 5
- [13] Ming Dai, Jian Li, Jiedong Zhuang, Xian Zhang, and Wankou Yang. Multi-task visual grounding with coarse-to-fine consistency constraints. In *Proceedings of the AAAI Conference on Artificial Intelligence*, pages 2618–2626, 2025. 6
- [14] Henghui Ding, Chang Liu, Suchen Wang, and Xudong Jiang. VLT: Vision-Language Transformer and Query Generation for Referring Segmentation. *IEEE Transactions on Pattern Analysis and Machine Intelligence (TPAMI)*, 45, 2023. 6
- [15] Haixin Ding, Shengchuan Zhang, Qiong Wu, Songlin Yu, Jie Hu, Liujuan Cao, and Rongrong Ji. Bilateral Knowledge Interaction Network for Referring Image Segmentation. *IEEE Transactions on Multimedia (TMM)*, 26, 2023. 6
- [16] Patrick Esser, Sumith Kulal, Andreas Blattmann, Rahim Entezari, Jonas Müller, Harry Saini, Yam Levi, Dominik Lorenz, Axel Sauer, Frederic Boesel, Dustin Podell, Tim Dockhorn, Zion English, Kyle Lacey, Alex Goodwin, Yan-nik Marek, and Robin Rombach. Scaling rectified flow transformers for high-resolution image synthesis. In *Proceedings of the 41st International Conference on Machine Learning (ICML)*, 2024. 2, 3, 4, 8
- [17] Patrick Esser, Sumith Kulal, Andreas Blattmann, Rahim Entezari, Jonas Müller, Harry Saini, Yam Levi, Dominik Lorenz, Axel Sauer, Frederic Boesel, Dustin Podell, Tim Dockhorn, Zion English, Kyle Lacey, Alex Goodwin, Yan-nik Marek, and Robin Rombach. Scaling rectified flow transformers for high-resolution image synthesis. In *Proceedings of the 41st International Conference on Machine Learning (ICML)*, 2024. 1
- [18] Mark Everingham, Luc Van Gool, Christopher K. I. Williams, John Winn, and Andrew Zisserman. The PASCAL visual object classes (VOC) challenge. *International Journal of Computer Vision*, 88(2):303–338, 2010. 6
- [19] Michael Fuest, Pingchuan Ma, Ming Gui, Johannes S. Fischer, Vincent Tao Hu, and Bjorn Ommer. Diffusion models and representation learning: A survey. *arXiv preprint arXiv:2407.00783*, 2024. 8
- [20] Frank Fundel, Johannes Schusterbauer, Vincent Tao Hu, and Björn Ommer. Distillation of diffusion features for semantic correspondence. In *IEEE/CVF Winter Conference on Applications of Computer Vision (WACV)*, 2025. 1, 8
- [21] Golnaz Ghiasi, Xiuye Gu, Yin Cui, and Tsung-Yi Lin. Scaling open-vocabulary image segmentation with image-level

- labels. In *European conference on computer vision*, pages 540–557. Springer, 2022. 1
- [22] Google DeepMind. Veo 3 tech report: Veo — a text-to-video generation system. Technical report, Google DeepMind, 2025. Technical report. 8
- [23] Jonathan Ho and Tim Salimans. Classifier-free diffusion guidance. In *NeurIPS 2021 Workshop on Deep Generative Models and Downstream Applications*, 2021. 6
- [24] Jonathan Ho, Ajay Jain, and Pieter Abbeel. Denoising diffusion probabilistic models. *Advances in neural information processing systems*, 33:6840–6851, 2020. 8
- [25] Yutao Hu, Qixiong Wang, Wenqi Shao, Enze Xie, Zhenguo Li, Jungong Han, and Ping Luo. Beyond One-to-One: Rethinking the Referring Image Segmentation. In *Proceedings of International Conference on Computer Vision (ICCV)*, 2023. 6
- [26] Sahar Kazemzadeh, Vicente Ordonez, Mark Matten, and Tamara Berg. ReferItGame: Referring to objects in photographs of natural scenes. In *Proceedings of the 2014 Conference on Empirical Methods in Natural Language Processing (EMNLP)*, 2014. 6
- [27] Seoyeon Kim, Minguk Kang, Dongwon Kim, Jaesik Park, and Suha Kwak. Extending clip’s image-text alignment to referring image segmentation. In *The North American Chapter of the Association for Computational Linguistics (NAACL)*, 2024. 1, 6
- [28] Xin Lai, Zhuotao Tian, Yukang Chen, Yanwei Li, Yuhui Yuan, Shu Liu, and Jiaya Jia. Lisa: Reasoning segmentation via large language model. In *Proceedings of the IEEE/CVF Conference on Computer Vision and Pattern Recognition (CVPR)*, 2024. 6, 7
- [29] Hsin-Ying Lee, Hung-Yu Tseng, Hsin-Ying Lee, and Ming-Hsuan Yang. Exploiting diffusion prior for generalizable dense prediction. In *Proceedings of the IEEE Conference on Computer Vision and Pattern Recognition (CVPR)*, 2024. 1, 8
- [30] Alexander C. Li, Mihir Prabhudesai, Shivam Duggal, Ellis Brown, and Deepak Pathak. Your diffusion model is secretly a zero-shot classifier. In *Proceedings of the IEEE/CVF International Conference on Computer Vision*, pages 2206–2217, 2023. 1, 8
- [31] Daiqing Li, Huan Ling, Seung Wook Kim, Karsten Kreis, Sanja Fidler, and Antonio Torralba. Bigdatasetgan: Synthesizing imagenet with pixel-wise annotations. In *Proceedings of the IEEE/CVF Conference on Computer Vision and Pattern Recognition*, pages 21330–21340, 2022. 8
- [32] Daiqing Li, Huan Ling, Amlan Kar, David Acuna, Seung Wook Kim, Karsten Kreis, Antonio Torralba, and Sanja Fidler. Dreamteacher: Pretraining image backbones with deep generative models. In *IEEE/CVF International Conference on Computer Vision (ICCV)*, 2023. 8
- [33] Feng Liang, Bichen Wu, Xiaoliang Dai, Kunpeng Li, Yinan Zhao, Hang Zhang, Peizhao Zhang, Peter Vajda, and Diana Marculescu. Open-vocabulary semantic segmentation with mask-adapted clip. In *Proceedings of the IEEE/CVF Conference on Computer Vision and Pattern Recognition*, pages 7061–7070, 2023. 7
- [34] Yaron Lipman, Ricky T. Q. Chen, Heli Ben-Hamu, Maximilian Nickel, and Matt Le. Flow matching for generative modeling. In *International Conference on Learning Representations (ICLR)*, 2023. 2
- [35] Chang Liu, Henghui Ding, and Xudong Jiang. Gres: Generalized referring expression segmentation. In *Proceedings of the IEEE/CVF Conference on Computer Vision and Pattern Recognition*, pages 23592–23601, 2023. 6
- [36] Jiang Liu, Hui Ding, Zhaowei Cai, Yuting Zhang, Ravi Kumar Satzoda, Vijay Mahadevan, and R. Manmatha. Polyformer: Referring image segmentation as sequential polygon generation. In *Proceedings of the IEEE/CVF conference on computer vision and pattern recognition*, pages 18653–18663, 2023. 6
- [37] Jinxiang Liu, Chen Ju, Chaofan Ma, Yanfeng Wang, Yu Wang, and Ya Zhang. Audio-aware query-enhanced transformer for audio-visual segmentation. *arXiv preprint arXiv:2307.13236*, 2023. 8
- [38] Jinxiang Liu, Yu Wang, Chen Ju, Chaofan Ma, Ya Zhang, and Weidi Xie. Annotation-free audio-visual segmentation. In *IEEE/CVF Winter Conference on Applications of Computer Vision (WACV)*, 2024. 8
- [39] Shiyu Liu, Yucheng Han, Peng Xing, Fukun Yin, Rui Wang, Wei Cheng, Jiaqi Liao, Yingming Wang, Honghao Fu, Chunrui Han, Guopeng Li, Yuang Peng, Quan Sun, Jingwei Wu, Yan Cai, Zheng Ge, Ranchen Ming, Lei Xia, Xianfang Zeng, Yibo Zhu, Binxing Jiao, Xiangyu Zhang, Gang Yu, and Daxin Jiang. Step1x-edit: A practical framework for general image editing. *arXiv preprint arXiv:2504.17761*, 2025. 5
- [40] Wentao Liu, Chaofan Ma, Yuhuan Yang, Weidi Xie, and Ya Zhang. Transforming the interactive segmentation for medical imaging. In *Medical Image Computing and Computer Assisted Intervention (MICCAI)*, 2022. 8
- [41] Xingchao Liu, Chengyue Gong, and Qiang Liu. Flow straight and fast: Learning to generate and transfer data with rectified flow. In *International Conference on Learning Representations (ICLR)*, 2023. 3
- [42] Grace Luo, Lisa Dunlap, Dong Huk Park, Aleksander Holynski, and Trevor Darrell. Diffusion hyperfeatures: Searching through time and space for semantic correspondence. In *Advances in Neural Information Processing Systems (NeurIPS)*, 2023. 1, 8
- [43] Chaofan Ma, Qisen Xu, Xiangfeng Wang, Bo Jin, Xiaoyun Zhang, Yanfeng Wang, and Ya Zhang. Boundary-aware supervoxel-level iteratively refined interactive 3d image segmentation with multi-agent reinforcement learning. *IEEE Transactions on Medical Imaging*, 40(10):2563–2574, 2021. 8
- [44] Chaofan Ma, Yuhuan Yang, Yanfeng Wang, Ya Zhang, and Weidi Xie. Open-vocabulary semantic segmentation with frozen vision-language models. In *British Machine Vision Conference (BMVC)*, 2022. 1
- [45] Chaofan Ma, Yuhuan Yang, Chen Ju, Fei Zhang, Jinxiang Liu, Yu Wang, Ya Zhang, and Yanfeng Wang. Diffusionseg: Adapting diffusion towards unsupervised object discovery. *arXiv preprint arXiv:2303.09813*, 2023. 1, 8

- [46] Chaofan Ma, Yuhuan Yang, Chen Ju, Fei Zhang, Ya Zhang, and Yanfeng Wang. Attrseg: Open-vocabulary semantic segmentation via attribute decomposition-aggregation. In *Advances in Neural Information Processing Systems*, 2023. 1
- [47] Chaofan Ma, Yuhuan Yang, Chen Ju, Yue Shi, Ya Zhang, and Yanfeng Wang. Freeseegdiff: Annotation-free saliency segmentation with diffusion models. In *IEEE International Conference on Acoustics, Speech and Signal Processing (ICASSP)*, 2025. 1
- [48] Jun Ma, Yuting He, Feifei Li, Lin Han, Chenyu You, and Bo Wang. Segment anything in medical images. *Nature Communications*, 15(1):654, 2024. 8
- [49] Zhenjie Mao, Yuhuan Yang, Chaofan Ma, Dongsheng Jiang, Jiangchao Yao, Ya Zhang, and Yanfeng Wang. Saffire: Saccade-fixation reiteration with mamba for referring image segmentation. In *Advances in Neural Information Processing Systems*, 2025. 6
- [50] Benyuan Meng, Qianqian Xu, Zitai Wang, Xiaochun Cao, and Qingming Huang. Not all diffusion model activations have been evaluated as discriminative features. In *Annual Conference on Neural Information Processing Systems*, pages 55141–55177, 2024. 1, 8
- [51] Varun K. Nagaraja, Vlad I. Morariu, and Larry S. Davis. Modeling context between objects for referring expression understanding. In *Computer Vision—ECCV 2016: 14th European Conference, Amsterdam, The Netherlands, October 11–14, 2016, Proceedings, Part IV 14*, pages 792–807. Springer, 2016. 6
- [52] Shuyi Ouyang, Hongyi Wang, Shiao Xie, Ziwei Niu, Ruofeng Tong, Yen-Wei Chen, and Lanfen Lin. SLViT: Scale-Wise Language-Guided Vision Transformer for Referring Image Segmentation. In *International Joint Conference on Artificial Intelligence (IJCAI)*, 2023. 6
- [53] William Peebles and Saining Xie. Scalable diffusion models with transformers. In *Proceedings of the IEEE/CVF International Conference on Computer Vision (ICCV)*, 2023. 5, 8
- [54] Dustin Podell, Zion English, Kyle Lacey, Andreas Blattmann, Tim Dockhorn, Jonas Müller, Joe Penna, and Robin Rombach. Sdxl: Improving latent diffusion models for high-resolution image synthesis. In *International Conference on Learning Representations (ICLR)*, 2024. 8
- [55] Alec Radford, Jong Wook Kim, Chris Hallacy, Aditya Ramesh, Gabriel Goh, Sandhini Agarwal, Girish Sastry, Amanda Askell, Pamela Mishkin, Jack Clark, et al. Learning transferable visual models from natural language supervision. In *International Conference on Machine Learning*, pages 8748–8763. PMLR, 2021. 1
- [56] Hanoona Rasheed, Muhammad Maaz, Sahal Shaji Mullaappilly, Abdelrahman Shaker, Salman Khan, Hisham Cholakkal, Rao M. Anwer, Eric Xing, Ming-Hsuan Yang, and Fahad S. Khan. Glamm: Pixel grounding large multimodal model. In *Proceedings of the IEEE/CVF Conference on Computer Vision and Pattern Recognition (CVPR)*, 2024. 7
- [57] Hanoona Rasheed, Muhammad Maaz, Sahal Shaji, Abdelrahman Shaker, Salman Khan, Hisham Cholakkal, Rao M. Anwer, Eric Xing, Ming-Hsuan Yang, and Fahad S. Khan. Glamm: Pixel grounding large multimodal model. In *Proceedings of the IEEE/CVF Conference on Computer Vision and Pattern Recognition (CVPR)*, 2024. 6
- [58] Tianhe Ren, Shilong Liu, Ailing Zeng, Jing Lin, Kunchang Li, He Cao, Jiayu Chen, Xinyu Huang, Yukang Chen, Feng Yan, et al. Grounded sam: Assembling open-world models for diverse visual tasks. *arXiv preprint arXiv:2401.14159*, 2024. 7
- [59] Zhongwei Ren, Zhicheng Huang, Yunchao Wei, Yao Zhao, Dongmei Fu, Jiashi Feng, and Xiaojie Jin. Pixellm: Pixel reasoning with large multimodal model. In *Proceedings of the IEEE/CVF Conference on Computer Vision and Pattern Recognition (CVPR)*, 2024. 6
- [60] Robin Rombach, Andreas Blattmann, Dominik Lorenz, Patrick Esser, and Björn Ommer. High-resolution image synthesis with latent diffusion models. In *Proceedings of the IEEE/CVF conference on computer vision and pattern recognition*, pages 10684–10695, 2022. 8
- [61] Robin Rombach, Andreas Blattmann, Dominik Lorenz, Patrick Esser, and Björn Ommer. High-resolution image synthesis with latent diffusion models. In *Proceedings of the IEEE/CVF Conference on Computer Vision and Pattern Recognition*, 2022. 1
- [62] Nisarg A. Shah, Vibashan VS, and Vishal M. Patel. Lqm-former: Language-aware query mask transformer for referring image segmentation. In *Proceedings of the IEEE/CVF Conference on Computer Vision and Pattern Recognition*, pages 12903–12913, 2024. 6
- [63] Chao Shang, Zichen Song, Heqian Qiu, Lanxiao Wang, Fanman Meng, and Hongliang Li. Prompt-driven referring image segmentation with instance contrasting. In *Proceedings of the IEEE/CVF Conference on Computer Vision and Pattern Recognition*, pages 4124–4134, 2024. 6
- [64] Nick Stracke, Stefan Andreas Baumann, Kolja Bauer, Frank Fundel, and Björn Ommer. Cleandift: Diffusion features without noise. In *Proceedings of the IEEE/CVF Conference on Computer Vision and Pattern Recognition*, 2025. 1, 8
- [65] Jiajin Tang, Ge Zheng, Cheng Shi, and Sibe Yang. Contrastive grouping with transformer for referring image segmentation. In *CVPR*, 2023. 6
- [66] Luming Tang, Menglin Jia, Qianqian Wang, Cheng Perng Phoo, and Bharath Hariharan. Emergent correspondence from image diffusion. In *Advances in Neural Information Processing Systems (NeurIPS)*, 2023. 1
- [67] Changyao Tian, Chenxin Tao, Jifeng Dai, Hao Li, Ziheng Li, Lewei Lu, Xiaogang Wang, Hongsheng Li, Gao Huang, and Xizhou Zhu. Addp: Learning general representations for image recognition and generation with alternating denoising diffusion process. In *International Conference on Learning Representations (ICLR)*, 2024. 8
- [68] Team Wan, Ang Wang, Baole Ai, Bin Wen, Chaojie Mao, Chen-Wei Xie, Di Chen, Feiwu Yu, Haiming Zhao, Jianxiao Yang, Jianyuan Zeng, Jiayu Wang, Jingfeng Zhang, Jingren Zhou, Jinkai Wang, Jixuan Chen, Kai Zhu, Kang Zhao, Keyu Yan, Lianghua Huang, Mengyang Feng, Ningyi Zhang, Pandeng Li, Pingyu Wu, Ruihang Chu, Ruili Feng, Shiwei

- Zhang, Siyang Sun, Tao Fang, Tianxing Wang, Tianyi Gui, Tingyu Weng, Tong Shen, Wei Lin, Wei Wang, Wei Wang, Wenmeng Zhou, Wenteng Wang, Wenting Shen, Wenyuan Yu, Xianzhong Shi, Xiaoming Huang, Xin Xu, Yan Kou, Yangyu Lv, Yifei Li, Yijing Liu, Yiming Wang, Yingya Zhang, Yitong Huang, Yong Li, You Wu, Yu Liu, Yulin Pan, Yun Zheng, Yuntao Hong, Yupeng Shi, Yutong Feng, Zeyinzi Jiang, Zhen Han, Zhi-Fan Wu, and Ziyu Liu. Wan: Open and advanced large-scale video generative models. *arXiv preprint arXiv:2503.20314*, 2025. 5, 6
- [69] Dianyi Wang, Ruihang Li, Feng Han, Chaofan Ma, Wei Song, Siyuan Wang, Yibin Wang, Yi Xin, Hongjian Liu, Zhixiong Zhang, Shengyuan Ding, Tianhang Wang, Zhenglin Cheng, Tao Lin, Cheng Jin, Kaicheng Yu, Jingjing Chen, Wenjie Wang, Zhongyu Wei, and Jiaqi Wang. Deepgen 1.0: A lightweight unified multimodal model for advancing image generation and editing. *arXiv preprint arXiv:2602.12205*, 2026. 8
- [70] Dianyi Wang, Chaofan Ma, Feng Han, Size Wu, Wei Song, Yibin Wang, Zhixiong Zhang, Tianhang Wang, Siyuan Wang, Zhongyu Wei, and Jiaqi Wang. Unireason 1.0: A unified reasoning framework for world knowledge aligned image generation and editing. *arXiv preprint arXiv:2602.02437*, 2026. 8
- [71] Zhaoqing Wang, Yu Lu, Qiang Li, Xunqiang Tao, Yandong Guo, Mingming Gong, and Tongliang Liu. CRIS: CLIP-Driven Referring Image Segmentation. In *IEEE Conference on Computer Vision and Pattern Recognition (CVPR)*, 2022. 1, 6
- [72] Zijie J. Wang, Evan Montoya, David Munechika, Haoyang Yang, Benjamin Hoover, and Duen Horng Chau. Diffusiondb: A large-scale prompt gallery dataset for text-to-image generative models. In *Proceedings of the 61st Annual Meeting of the Association for Computational Linguistics (ACL)*, 2023. 6
- [73] Chenyuan Wu, Pengfei Zheng, Ruiran Yan, Shitao Xiao, Xin Luo, Yueze Wang, Wanli Li, Xiyan Jiang, Yexin Liu, Junjie Zhou, Ze Liu, Ziyi Xia, Chaofan Li, Haoge Deng, Jiahao Wang, Kun Luo, Bo Zhang, Defu Lian, Xinlong Wang, Zhongyuan Wang, Tiejun Huang, and Zheng Liu. Omnigen2: Exploration to advanced multimodal generation. *arXiv preprint arXiv:2506.18871*, 2025. 8
- [74] Zhuofan Xia, Dongchen Han, Yizeng Han, Xuran Pan, Shiji Song, and Gao Huang. Gsva: Generalized segmentation via multimodal large language models. In *Proceedings of the IEEE/CVF Conference on Computer Vision and Pattern Recognition*, pages 3858–3869, 2024. 6
- [75] Weilai Xiang, Hongyu Yang, Di Huang, and Yunhong Wang. Denoising diffusion autoencoders are unified self-supervised learners. In *IEEE/CVF International Conference on Computer Vision (ICCV)*, 2023. 8
- [76] Linhui Xiao, Xiaoshan Yang, Fang Peng, Yaowei Wang, and Changsheng Xu. Oneref: Unified one-tower expression grounding and segmentation with mask referring modeling. *Advances in Neural Information Processing Systems*, 37:139854–139885, 2024. 6
- [77] Jiarui Xu, Shalini De Mello, Sifei Liu, Wonmin Byeon, Thomas Breuel, Jan Kautz, and Xiaolong Wang. Groupvit: Semantic segmentation emerges from text supervision. In *Proceedings of the IEEE/CVF conference on computer vision and pattern recognition*, pages 18134–18144, 2022. 1
- [78] Jiarui Xu, Sifei Liu, Arash Vahdat, Wonmin Byeon, Xiaolong Wang, and Shalini De Mello. Open-vocabulary panoptic segmentation with text-to-image diffusion models. In *Proceedings of the IEEE/CVF Conference on Computer Vision and Pattern Recognition (CVPR)*, 2023. 1, 8
- [79] Jinjin Xu, Liwu Xu, Yuzhe Yang, Xiang Li, Yanchun Xie, Yi-Jie Huang, and Yaqian Li. u-llava: Unifying multi-modal tasks via large language model. In *European Conference on Artificial Intelligence (ECAI)*, 2024. 6
- [80] Bin Yan, Yi Jiang, Jiannan Wu, Dong Wang, Ping Luo, Zehuan Yuan, and Huchuan Lu. Universal instance perception as object discovery and retrieval. In *Proceedings of the IEEE/CVF Conference on Computer Vision and Pattern Recognition*, pages 15325–15336, 2023. 6
- [81] Xingyi Yang and Xinchao Wang. Diffusion model as representation learner. In *IEEE/CVF International Conference on Computer Vision (ICCV)*, 2023. 8
- [82] Xingyi Yang and Xinchao Wang. Diffusion model as representation learner. In *Proceedings of the IEEE/CVF International Conference on Computer Vision (ICCV)*, 2023. 1
- [83] Xiulong Yang, Sheng-Min Shih, Yinlin Fu, Xiaoting Zhao, and Shihao Ji. Your vit is secretly a hybrid discriminative-generative diffusion model. *arXiv preprint arXiv:2208.07791*, 2022. 8
- [84] Yuhuan Yang, Chaofan Ma, Chen Ju, Fei Zhang, Jiangchao Yao, Ya Zhang, and Yanfeng Wang. Multi-modal prototypes for open-world semantic segmentation. *International Journal of Computer Vision*, 2024. 1
- [85] Yuhuan Yang, Chaofan Ma, Jiangchao Yao, Zhun Zhong, Ya Zhang, and Yanfeng Wang. Remember: Referring image segmentation with mamba twister. In *European Conference on Computer Vision (ECCV)*, pages 108–126, 2024. 6
- [86] Yuhuan Yang, Chaofan Ma, Zhenjie Mao, Jiangchao Yao, Ya Zhang, and Yanfeng Wang. Moma: Modulating mamba for adapting image foundation models to video recognition. In *International Conference on Machine Learning (ICML)*, 2025. 5
- [87] Zhao Yang, Jiaqi Wang, Yansong Tang, Kai Chen, Hengshuang Zhao, and Philip H. S. Torr. LAVT: Language-Aware Vision Transformer for Referring Image Segmentation. In *IEEE Conference on Computer Vision and Pattern Recognition (CVPR)*, 2022. 6
- [88] Zhao Yang, Jiaqi Wang, Yansong Tang, Kai Chen, Hengshuang Zhao, and Philip H. S. Torr. Semantics-Aware Dynamic Localization and Refinement for Referring Image Segmentation. In *AAAI Conference on Artificial Intelligence (AAAI)*, 2023. 6
- [89] Fei Zhang, Tianfei Zhou, Boyang Li, Hao He, Chaofan Ma, Tianjiao Zhang, Jiangchao Yao, Ya Zhang, and Yanfeng Wang. Uncovering prototypical knowledge for weakly open-vocabulary semantic segmentation. In *Advances in Neural Information Processing Systems*, 2023. 1
- [90] Yuxuan Zhang, Huan Ling, Jun Gao, Kangxue Yin, Jean-Francois Lafleche, Adela Barriuso, Antonio Torralba, and

- Sanja Fidler. Datasetgan: Efficient labeled data factory with minimal human effort. In *Proceedings of the IEEE/CVF Conference on Computer Vision and Pattern Recognition*, pages 10145–10155, 2021. [8](#)
- [91] Zheng Zhang, Yeyao Ma, Enming Zhang, and Xiang Bai. Psalm: Pixelwise segmentation with large multi-modal model. In *European Conference on Computer Vision (ECCV)*, pages 74–91, 2024. [6](#)
- [92] Wenliang Zhao, Yongming Rao, Zuyan Liu, Benlin Liu, Jie Zhou, and Jiwen Lu. Unleashing text-to-image diffusion models for visual perception. In *Proceedings of the IEEE/CVF International Conference on Computer Vision*, pages 5729–5739, 2023. [8](#)
- [93] Bolei Zhou, Hang Zhao, Xavier Puig, Tete Xiao, Sanja Fidler, Adela Barriuso, and Antonio Torralba. Semantic understanding of scenes through the ade20k dataset. *International Journal of Computer Vision*, 127:302–321, 2019. [6](#)
- [94] Jinxing Zhou, Jianyuan Wang, Jiayi Zhang, Weixuan Sun, Jing Zhang, Stan Birchfield, Dan Guo, Lingpeng Kong, Meng Wang, and Yiran Zhong. Audio-visual segmentation. In *European Conference on Computer Vision (ECCV)*, pages 386–403, 2022. [8](#)
- [95] Xueyan Zou, Jianwei Yang, Hao Zhang, Feng Li, Linjie Li, Jianfeng Wang, Lijuan Wang, Jianfeng Gao, and Yong Jae Lee. Segment everything everywhere all at once. In *Advances in Neural Information Processing Systems (NeurIPS)*, 2023. [7](#)